
Proceedings Paper:
Li, X., Yang, L., Mihaylova, L.S. orcid.org/0000-0001-5856-2223 et al. (2 more authors) (2018) Enhanced GMM-based Filtering with Measurement Update Ordering and Innovation-based Pruning. In: Proceedings of the International Conference on Information Fusion. International Conference on Information Fusion, 13 Jul 2018 - 13 Jul 2017, Cambridge, UK. IEEE . ISBN 978-0-9964527-6-2

10.23919/ICIF.2018.8455666

Enhanced GMM-based Filtering with Measurement Update Ordering and Innovation-based Pruning

Xi Li[1,2], Le Yang[2,4], Lyudmila Mihaylova[3], Fucheng Guo[1], Min Zhang[1]
1. School of Electronic Science, National University of Defense Technology, Changsha China
2. School of Internet of Things (IoT) Engineering, Jiangnan University, Wuxi China
3. Department of Automatic Control & System Engineering, University of Sheffield, Sheffield UK
4. Department of ECE, University of Canterbury, Christchurch, New Zealand

***Abstract*—The use of Gaussian mixture model (GMM) in nonlinear/non-Gaussian filtering problems has been extensively investigated. This paper advocates two enhancements for GMM-based nonlinear filtering techniques, namely, the adaptive ordering of the measurement update and normalized innovation square (NIS)-based mixture component management. The former technique selects the order of measurement update that maximizes the marginal measurement likelihood to improve performance. The latter takes the filtering history of a mixture component into account and prunes those components with NIS larger than a threshold to eliminate their impact on the filtering posterior. The advantage of the proposed enhancements is illustrated via simulations that consider source tracking using the time difference of arrival (TDOA) and frequency difference of arrival (FDOA) measurements received at two unmanned aerial vehicles (UAVs). A GMM-cubature quadrature Kalman filter (CQKF) is implemented and its performances with different measurement update and mixture component management strategies are compared. The superior performance obtained via the use of the two proposed techniques is demonstrated.**

I. Introduction

The problem of nonlinear/non-Gaussian Bayesian filtering arises frequently in e.g., target tracking applications. The optimal solution to this problem, according to the minimum mean square error (MMSE) criterion, is known to be the conditional mean of the state posterior distribution [1]. However, the nonlinearity and/or non-Gaussianity in the filtering problems may render obtaining closed-form state estimates infeasible.

To address the above difficulty, a number of suboptimal but mathematically tractable filtering methods have been developed. Among them, the particle filtering (PF) [1] approaches can provide *global* approximation to the optimal solutions. They are computationally expensive and could suffer from the curse of dimensionality when handling high-dimensional problems [2]. On the other hand, the Kalman filter (KF)-based methods [3], [4] have lower computation burden. But only *local* approximations of the optimal solutions can be obtained as they often assume Gaussian prior and posterior distributions. This assumption may be violated in practice, which would lead to degraded performance especially when the system nonlinearity becomes severe.

The Gaussian mixture model (GMM)-based methods [5] are known to have a better tradeoff between the computational cost and filtering accuracy. They maintain multiple nonlinear KF filters, also known as Gaussian components, to cover the state space. The Gaussian components are running in parallel, each of which is associated with a weight. The GMM filter combines the estimates from all the components to produce its state estimate. Splitting the Gaussian components can further reduce the system nonlinearity and improve performance. But this would increase the number of mixture components exponentially over time. The use of appropriate mixture reduction (MR) schemes [6] is therefore essential for making the GMM-based tracking methods practically applicable.

The decisions of the MR module on which components are pruned or merged may have significant impact on the filtering performance. Existing MR methods, which will be briefly surveyed in Section II, consider the structure of the mixture distribution at the current sampling time only. Whether the Gaussian component has yielded a *consistent* estimate of the state over time is not taken into account. In particular, if KF filters that produce inconsistent results are propagated further, significant performance degradation or even filtering divergence can occur. As a result, new MR schemes that are based at least partially on the *filtering history* of the mixture components would be beneficial for GMM-based tracking.

Another important aspect in nonliner/non-Gaussian filtering is the measurement update order with which the measurements at each sampling time are utilized in a *sequential* manner instead of being exploited together. It is preferable to determine for each component an update order such that its weight, which is indeed proportional to the marginal measurement likelihood, is enlarged for improved tracking accuracy.

We shall propose in this paper two enhancements for the GMM-based filtering methods. Specifically, an innovation-based mixture pruning technique that removes Gaussian components with inconsistent state estimation results is developed. This scheme is found to be able to help preserve the components that yield estimates close to the true solutions in the mixture. Another enhancement is the adaptive measurement update ordering technique. It is incorporated into every Gaussian component such that the component weight after measurement update would be maximized.

We demonstrate the effectiveness of the two proposed enhancements via developing a GMM-based cubature quadrature Kalman filter (CQKF). The resulting GMM-CQKF algorithm with different measurement update ordering and MR strategies is applied to track a moving source using the time

difference of arrival (TDOA) and frequency difference of arrival (FDOA) measurements obtained at two unmanned aerial vehicles (UAVs). Extensive simulation experiments are conducted. They verify that the two proposed methods can offer performance improvements in terms of better tracking accuracy and smaller track loss probability over alternative measurement update ordering and MR schemes.

The remainder of this paper is organized as follows. Section II reviews the related works with a focus on MR. Section III introduces the CQKF algorithm, a recently developed nonlinear KF [7]. Section IV presents the GMM-CQKF algorithm with the adaptive measurement update ordering and innovation-based mixture pruning. Section V provides the simulation results. The conclusions are given in Section VI.

II. Related Works on Mixture Reduction

In the GMM-based filtering, MR techniques are adopted in order to prevent the exponential increase in the number of mixture components [8]. The principle behind most MR methods is to find, via least modifications, a new mixture with a limited number of components from the original one. In the literature, there exist quite a few MR methods. Among them, pruning is perhaps the most straightforward approach to control the number of components. But it is subject to the loss of information and may cause filtering divergence because eliminating components could lead to insufficient coverage of the state space. Besides pruning, a more sophisticated way is to merge multiple components into one to achieve MR [9]. The selection of components for merging can be based on minimizing some cost functions or distance measure. We shall briefly review several commonly used MR algorithms in the rest of this section.

Suppose at time k, the state posterior distribution is approximated using a weighted sum of M_k Gaussian components as

$$p(\mathbf{x}_k|\mathbf{Z}^k) = \sum_{j=1}^{M_k} w_k^j \mathcal{N}(\mathbf{x}_k|\hat{\mathbf{x}}_{k|k}^j, \mathbf{P}_{k|k}^j) \tag{1}$$

where $\mathbf{x}_k$ is the state vector at time k. $\mathbf{Z}^k = \{\mathbf{z}_1, \mathbf{z}_2, \ldots, \mathbf{z}_k\}$ collects the measurements available up to time k, where $\mathbf{z}_i$, $i = 1, 2, ...k$, is the measurement vector at time i. $\hat{\mathbf{x}}_{k|k}^j$ and $\mathbf{P}_{k|k}^j$ denote separately the mean vector and covariance matrix of the jth Gaussian component. w_k^j is the weight of component j and they satisfy $\sum_{j=1}^{M_k} w_k^j = 1$. In this work, we use $\mathcal{N}(\mathbf{x}|\boldsymbol{\mu}, \boldsymbol{\Sigma})$ to represent that the random vector $\mathbf{x}$ follows the Gaussian distribution with mean vector $\boldsymbol{\mu}$ and covariance matrix $\boldsymbol{\Sigma}$. The objective is to approximate the mixture on the right hand side (RHS) of (1) using $N_{max}(N_{max} < M_k)$ Gaussian components.

In [10], Salmond developed the joining algorithm for MR. The two components that minimize the following distance

$$d_{ij,k}^2 = \frac{w_k^i w_k^j}{w_k^i + w_k^j} (\hat{\mathbf{x}}_{k|k}^i - \hat{\mathbf{x}}_{k|k}^j)^T \mathbf{P}_{k|k}^{-1} (\hat{\mathbf{x}}_{k|k}^i - \hat{\mathbf{x}}_{k|k}^j) \tag{2}$$

are merged, where $i, j = 1, 2, ..., M_k$. $\mathbf{P}_{k|k}$ denotes the sample covariance of $\mathbf{x}_k$, which is given by, from (1),

$$\mathbf{P}_{k|k} = \sum_{j=1}^{M_k} w_k^j [\mathbf{P}_{k|k}^j + \hat{\mathbf{x}}_{k|k}^j (\hat{\mathbf{x}}_{k|k}^j)^T] - \hat{\mathbf{x}}_{k|k} \hat{\mathbf{x}}_{k|k}^T. \tag{3}$$

$\hat{\mathbf{x}}_{k|k}$ is the sample mean of $\mathbf{x}_k$, which is equal to

$$\hat{\mathbf{x}}_{k|k} = \sum_{j=1}^{M_k} w_k^j \hat{\mathbf{x}}_{k|k}^j. \tag{4}$$

We can deduce from (2) that the joining method [10] tends to merge components with low weights or mean vectors close to each other.

[11] proposed an integral square difference (ISD)-based technique. It can choose either component pruning or merging, depending on the original mixture distribution. The ISD cost function is in closed form but the parameters of the new mixture can only be found via iterative numerical optimization. Convergence to the globally optimal solution is not guaranteed. Alternative MR method that exploits the statistical decision theory is available in [12].

Similarity-based MR methods were developed in [6], [9], [13]. In particular, [6] suggested a Kullback-Leibler (KL) divergence-based similarity measure such that the component pair selected for merging is the one minimizing

$$\begin{aligned} D_{ij,k} = \frac{1}{2}[&(w_k^i + w_k^j) \log\det(\mathbf{P}_{k|k}^{ij}) \\ &- w_k^i \log\det(\mathbf{P}_{k|k}^i) - w_k^j \log\det(\mathbf{P}_{k|k}^j)]. \end{aligned} \tag{5}$$

Here, the covariance matrix $\mathbf{P}_{k|k}^{ij}$ is equal to

$$\begin{aligned} \mathbf{P}_{k|k}^{ij} =& w_k^{i|ij} \mathbf{P}_{k|k}^i + w_k^{j|ij} \mathbf{P}_{k|k}^j \\ &+ w_k^{i|ij} w_k^{j|ij} (\hat{\mathbf{x}}_{k|k}^i - \hat{\mathbf{x}}_{k|k}^j)(\hat{\mathbf{x}}_{k|k}^i - \hat{\mathbf{x}}_{k|k}^j)^T \end{aligned} \tag{6}$$

$w_k^{i|ij} = w_k^i/(w_k^i + w_k^j)$ and $w_k^{i|ij} + w_k^{j|ij} = 1$. With the above cost function, the two components having low weights, mean vectors near to each other or similar covariance matrices would tend to be merged [6].

In [9], another similarity measure is given by

$$S_{ij,k}^2 = \frac{\mathcal{N}(\mathbf{0}|\hat{\mathbf{x}}_{k|k}^i, 0.5\mathbf{P}_{k|k}^i)\mathcal{N}(\mathbf{0}|\hat{\mathbf{x}}_{k|k}^j, 0.5\mathbf{P}_{k|k}^j)}{\mathcal{N}(\mathbf{0}|\hat{\mathbf{x}}_{k|k}^{ij}, \mathbf{P}_{k|k}^{ij})^2}. \tag{7}$$

$\hat{\mathbf{x}}_{k|k}^{ij}$ and $\mathbf{P}_{k|k}^{ij}$ represent separately the product mean vector and covariance matrix of Gaussian components i and j. They are defined as

$$\mathbf{P}_{k|k}^{ij} = [(\mathbf{P}_{k|k}^i)^{-1} + (\mathbf{P}_{k|k}^j)^{-1}]^{-1} \tag{8}$$

$$\hat{\mathbf{x}}_{k|k}^{ij} = \mathbf{P}_{k|k}^{ij} [(\mathbf{P}_{k|k}^i)^{-1} \hat{\mathbf{x}}_{k|k}^i + (\mathbf{P}_{k|k}^j)^{-1} \hat{\mathbf{x}}_{k|k}^j]. \tag{9}$$

The component pair that maximizes (7) is selected for merging. A potential drawback of this approach lies in the fact that the similarity measure (7) does not take into account the weights of the components.

Apart from the pairwise MR methods described above, there exist techniques that merge at least three Gaussian components

at a time, such as the one developed in [14] that chooses several components with small weights for merging. However, these methods may introduce significant bias if the mean vectors of the chosen components are distant from one another. To address this weakness, MR methods that utilizes clustering algorithms when merging multiple components have been developed in [10] and [15]. The progressive MR approaches can be found in [16]. For a more comprehensive review of the MR methods, interested readers can refer to [17].

III. Cubature Quadrature Kalman Filter

We shall illustrate the CQKF algorithm via showing its application in estimating the state of the following state-space model with additive process and measurement noises

$$\mathbf{x}_k = \mathbf{f}_k(\mathbf{x}_{k-1}) + \mathbf{n}_k \tag{10}$$

$$z_k^i = h_k^i(\mathbf{x}_k) + v_k^i, \quad i = 1, 2, \ldots, n_z. \tag{11}$$

$\mathbf{x}_k$ is the unknown state vector at time k to be identified. $\mathbf{f}_k(\cdot)$ is the state propagation function, which could be nonlinear with respect to $\mathbf{x}_{k-1}$. $\mathbf{n}_k$ is the process noise assumed to be white Gaussian with zero mean and known covariance matrix $\mathbf{Q}_k$. The system has n_z measurements at time k and we collect them as $\mathbf{z}_k = [z_k^1, z_k^2, \ldots, z_k^{n_z}]^T$. The ith measurement z_k^i has a true value $h_k^i(\mathbf{x}_k)$, which could also be nonlinearly related to $\mathbf{x}_k$. The measurement noise v_k^i is zero-mean Gaussian distributed with variance $\sigma_{i,k}^2$. We further assume that the measurement noises are independent to one another[1].

The recently developed CQKF [7] estimates $\mathbf{x}_k$ using all the available measurements up to time k and the state-space model given in (10) and (11). Specifically, it exploits the third-order spherical-cubature rule and Gauss-Laguerre quadrature rule to evaluate numerically the integrals involved in the optimal Bayesian filtering (BF). It has been shown [7] that the performance of CQKF is comparable to these of the existing numerical integral-based nonlinear KFs such as the cubature KF (CKF) [4], [18], Gauss-Hermite KF (GHKF) [3] and stochastic integration filter (SIF) [19]. Furthermore, its filtering accuracy can improve with adopting higher-order quadrature rules. The CQKF relies on the well-known prediction-update recursion for state estimation, as other nonlinear KFs.

A. CQ Points

The CQKF filter works with a set of weighted cubature quadrature (CQ) points. The number of CQ points increases linearly with the dimension of the state $\mathbf{x}_k$, denoted by n_x. The CQ points $\boldsymbol{\xi}_l$ and corresponding weights $\bar{w}_l$ are obtained using

$$\boldsymbol{\xi}_l = \sqrt{2\delta_m}\boldsymbol{\zeta}_{m'} \tag{12}$$

$$\bar{w}_l = \frac{n_d!\Gamma(\varphi + n_d + 1)}{2n_x\delta_m\Gamma(n_x/2)[\dot{L}_{n_d}^{\varphi}(\delta_m)]^2}. \tag{13}$$

[1]When the measurement noises v_k^i are correlated, pre-whitening can be performed such that a linearly transformed version of the measurements would have independent noises.

$\boldsymbol{\zeta}_{m'}$ is the cubature point from the third-order spherical-cubature rule, which is equal to

$$\boldsymbol{\zeta}_{m'} = [\mathbf{I}_{n_x}, -\mathbf{I}_{n_x}]_{m'}, \quad m' = 1, 2, \ldots, 2n_x \tag{14}$$

where $[\mathbf{A}]_{m'}$ represents the m'th column of the matrix $\mathbf{A}$, and $\mathbf{I}_{n_x}$ is a $n_x \times n_x$ identity matrix. The quadrature point δ_m in (12) is the mth root of the n_d-order Chebyshev-Laguerre polynomial

$$\begin{aligned} L_{n_d}^{\varphi}(\delta) =& \delta^{n_d} - \frac{n_d}{1!}(n_d + \varphi)\delta^{n_d - 1} + \frac{n_d(n_d - 1)}{2!} \\ & \times (n_d + \varphi)(n_d + \varphi - 1)\delta^{n_d - 2} - \ldots = 0 \end{aligned} \tag{15}$$

where $\varphi = (n_x/2 - 1)$, $m = 1, 2, \ldots, n_d$ and $l = 1, 2, \ldots, L$. $\dot{L}_{n_d}^{\varphi}(\delta_m)$ is the first-order derivative of $L_{n_d}^{\varphi}(\delta_m)$ with respect to δ_m. The required number of CQ points is $L = 2n_x n_d$ when the n_d-order Gauss-Laguerre quadrature rule is used.

B. CQKF Prediction

Similar to other nonlinear KFs, CQKF assumes Gaussianity for the state posterior. Suppose $\hat{\mathbf{x}}_{k-1|k-1}^j$ is the mean vector of the state estimate at previous time $k-1$ and $\mathbf{P}_{k-1|k-1}^j = \mathbf{S}_{k-1}^j(\mathbf{S}_{k-1}^j)^T$ is its covariance matrix. CQKF achieves the state prediction via

$$\boldsymbol{\mu}_{k-1|k-1}^{l,j} = \mathbf{S}_{k-1}^j\boldsymbol{\xi}_l + \hat{\mathbf{x}}_{k-1|k-1}^j \tag{16}$$

$$\boldsymbol{\mu}_{k|k-1}^{l,j} = \mathbf{f}_k(\boldsymbol{\mu}_{k-1|k-1}^{l,j}) \tag{17}$$

$$\hat{\mathbf{x}}_{k|k-1}^j = \sum_{l=1}^{L} \bar{w}_l\boldsymbol{\mu}_{k|k-1}^{l,j} \tag{18}$$

$$\mathbf{P}_{k|k-1}^j = \sum_{l=1}^{L} \bar{w}_l(\boldsymbol{\mu}_{k|k-1}^{l,j} - \hat{\mathbf{x}}_{k|k-1}^j)(\boldsymbol{\mu}_{k|k-1}^{l,j} - \hat{\mathbf{x}}_{k|k-1}^j)^T + \mathbf{Q}_k \tag{19}$$

where $\hat{\mathbf{x}}_{k|k-1}^j$ is the predictive mean of the current state vector $\mathbf{x}_k$ and $\mathbf{P}_{k|k-1}^j = \mathbf{S}_{k|k-1}^j(\mathbf{S}_{k|k-1}^j)^T$ is the predictive covariance matrix.

C. CQKF Measurement Update

The measurements can be utilized with an *arbitrary* order to update the predictive distribution of $\mathbf{x}_k$ to produce its posterior distribution. Alternatively, they can be exploited in a joint manner as in [7]. We shall present the measurement update of CQKF using the measurement z_k^i. Subsequent measurement updates using the remaining measurements follow similarly.

First, the predicted measurement $\hat{z}_{k|k-1}^{i,j}$ is calculated using

$$\boldsymbol{\alpha}_{k|k-1}^{l,j} = \mathbf{S}_{k|k-1}^j\boldsymbol{\xi}_l + \hat{\mathbf{x}}_{k|k-1}^j \tag{20}$$

$$\beta_{k|k-1}^{l,j} = h_k^i(\boldsymbol{\alpha}_{k|k-1}^{l,j}) \tag{21}$$

$$\hat{z}_{k|k-1}^{i,j} = \sum_{l=1}^{L} \bar{w}_l\beta_{k|k-1}^{l,j}. \tag{22}$$

The Kalman gain is

$$\mathbf{G}_k^{i,j} = \mathbf{P}_{xz,k}^{i,j}(\mathbf{P}_{zz,k}^{i,j})^{-1} \tag{23}$$

where the cross covariance $\mathbf{P}_{xz,k}^{i,j}$ and the innovation covariance $\mathbf{P}_{zz,k}^{i,j}$ are equal to

$$\mathbf{P}_{xz,k}^{i,j} = \sum_{l=1}^{L} \bar{w}_l (\boldsymbol{\alpha}_{k|k-1}^{l,j} - \hat{\mathbf{x}}_{k|k-1}^{j})(\beta_{k|k-1}^{l,j} - \hat{z}_{k|k-1}^{i,j}) \quad (24)$$

$$\mathbf{P}_{zz,k}^{i,j} = \sum_{l=1}^{L} \bar{w}_l (\beta_{k|k-1}^{l,j} - \hat{z}_{k|k-1}^{i,j})^2 + \sigma_{i,k}^2. \quad (25)$$

The state posterior mean and covariance can then be found using their predictive version, $\hat{\mathbf{x}}_{k|k-1}^{j}$ and $\mathbf{P}_{k|k-1}^{j}$, as well as the Kalman gain $\mathbf{G}_k^{i,j}$, the measurement z_k^i and predictive measurement $\hat{z}_{k|k-1}^{i,j}$. They are given by

$$\hat{\mathbf{x}}_{k|k}^{i,j} = \hat{\mathbf{x}}_{k|k-1}^{j} + \mathbf{G}_k^{i,j}(z_k^i - \hat{z}_{k|k-1}^{i,j}) \quad (26)$$

$$\mathbf{P}_{k|k}^{i,j} = \mathbf{P}_{k|k-1}^{j} - \mathbf{G}_k^{i,j}\mathbf{P}_{zz,k}^{i,j}(\mathbf{G}_k^{i,j})^T. \quad (27)$$

$\hat{\mathbf{x}}_{k|k}^{i,j}$ is the posterior mean and $\mathbf{P}_{k|k}^{i,j}$ is the posterior covariance matrix after the measurement update using z_k^i is carried out.

To perform measurement update using another measurement, we just need to replace $\hat{\mathbf{x}}_{k|k-1}^{j}$ with $\hat{\mathbf{x}}_{k|k}^{i,j}$ and $\mathbf{P}_{k|k-1}^{j}$ with $\mathbf{P}_{k|k}^{i,j}$, and then repeat (20) $\sim$ (27).

IV. GMM-CQKF with Measurement Update Ordering and Innovation-based Pruning

As pointed out in the previous section, the CQKF approximates the posterior distribution of the state using a single multivariate Gaussian distribution. This may degrade its performance in handling filtering problems with severe nonlinearity and/or non-Gaussianity. In this section, we shall incorporate the GMM framework so that a GMM-CQKF filter can be obtained, which has better approximation of the state posterior with multiple Gaussian components.

Under the GMM-CQKF, the state posterior at previous time $k-1$ may be expressed as the following Gaussian mixture with N_{k-1} components

$$p(\mathbf{x}_{k-1}|\mathbf{Z}^{k-1}) = \sum_{j=1}^{N_{k-1}} w_{k-1}^{j} \mathcal{N}(\mathbf{x}_{k-1}|\hat{\mathbf{x}}_{k-1|k-1}^{j}, \mathbf{P}_{k-1|k-1}^{j}) \quad (28)$$

where $\hat{\mathbf{x}}_{k-1|k-1}^{j}$ and $\mathbf{P}_{k-1|k-1}^{j}$ represent the state mean vector and covariance matrix of the jth component. The weights w_{k-1}^{j} are normalized such that $\sum_{j=1}^{N_{k-1}} w_{k-1}^{j} = 1$.

The GMM-CQKF also adopts the prediction-update recursion to calculate the state posterior at time k using the state posterior at time $k-1$, n_z newly obtained measurements in $\mathbf{z}_k = [z_k^1, z_k^2, \ldots, z_k^{n_z}]^T$, and the state-space model in (10) and (11). Each Gaussian component of the GMM-CQKF carries out its state prediction in parallel. In particular, the state prediction of the jth component yields the predicted mean vector $\hat{\mathbf{x}}_{k|k-1}^{j}$ and covariance matrix $\mathbf{P}_{k|k-1}^{j}$ by following (16) $\sim$ (19), where $j = 1, 2, ..., N_{k-1}$.

We shall next present the measurement update of the GMM-CQKF, which is enhanced with a proposed measurement update ordering scheme, and the MR for the GMM-CQKF, which is a newly proposed technique based on the innovation.

A. GMM-CQKF Measurement Update

The measurement update needs to be performed at *every* component using the *same* measurements in $\mathbf{z}_k$. The associated processing has been described in Section III.C where the measurements are utilized in an *arbitrary* order. Here, we shall introduce an enhancement for measurement update in GMM-CQKF, the determination of the measurement update order that maximizes the component weight. The measurement update of GMM-CQKF ends with splitting components with large weights, which is aimed at reducing the nonlinearity and non-Gaussianity of the filtering problem to improve performance.

1) Measurement Update Ordering: Theoretically, under the framework of optimal Bayesian filtering, carrying out measurement update in *any* order should lead to the same state posterior distribution [5]. However, this is no longer valid in practice when the measurement is nonlinearly related to the state and nonlinear KFs such as the CQKF is adopted for state estimation. This is because after the measurement update using one particular measurement, the state posterior would be approximated using a Gaussian distribution, causing an approximation error. As a result, different measurement ordering can result in different approximation errors and discrepant filtering outcomes. To enhance the filtering accuracy of GMM-CQKF, we propose to determine the optimal measurement update order for each component.

There are in total $n_z!$ possible measurement update orders. But for each component, we shall use the one that maximizes the corresponding component weight after the measurement update. If n_z is high, the computation cost can be large. But for a small value of n_z, an exhaustive search can be carried out and the proposed measurement update scheme for the jth component is summarized in Algorithm 1.

2) Component Splitting: Splitting a Gaussian component normally refers to decreasing the system nonlinearity and non-Gaussianity through covering the most likely area in the state space with more components. For this purpose, in the developed GMM-CQKF, we choose the component whose weight after measurement update is the largest for component splitting. To prevent excessive increase in the computational cost, the component splitting is only executed when the number of components N_{k-1} is smaller than some pre-specified value N_{max}.

Suppose after the measurement update the tth component has the largest weight w_k^t and it is selected for splitting. The idea is to split its *predictive* distribution $\mathcal{N}(\mathbf{x}_k|\hat{\mathbf{x}}_{k|k-1}^{t}, \mathbf{P}_{k|k-1}^{t})$ into multiple Gaussian components and then carry out the measurement update for each new component *again*. To reduce modification in the mixture structure due to component splitting, we assume that the predictive distribution of the tth component can be approximated via

$$\begin{aligned} &\mathcal{N}(\mathbf{x}_k|\hat{\mathbf{x}}_{k|k-1}^{t}, \mathbf{P}_{k|k-1}^{t}) \approx \\ &\quad w_c \mathcal{N}(\mathbf{x}_k|\hat{\mathbf{x}}_{k|k-1}^{t}, \mathbf{P}_{k|k-1}^{t}) + w_p \mathcal{N}(\mathbf{x}_k|\hat{\mathbf{x}}_p, \mathbf{P}_p) \end{aligned} \quad (29)$$

where $\hat{\mathbf{x}}_p = \hat{\mathbf{x}}_{k|k-1}^{t}$, $\mathbf{P}_p = \kappa^2 \mathbf{P}_{k|k-1}^{t}$ ($\kappa > 1$), $w_c = 1 - w_p$ and $w_p \approx 0$.

Algorithm 1: Optimal Measurement Update Ordering Determination

Input: $\mathbf{z}_k, \hat{\mathbf{x}}^j_{k|k-1}, \mathbf{P}^j_{k|k-1}, w^j_{k-1}$

Output: $\hat{\mathbf{x}}^j_{k|k}, \mathbf{P}^j_{k|k}, w^j_k, \epsilon^j_k$

1 Initialize $\mathbf{d}_1 = [1, 2, \ldots, n_z]^T$

2 Set $\boldsymbol{\mu}_0 = \hat{\mathbf{x}}^j_{k|k-1}$, $\boldsymbol{\Sigma}_0 = \mathbf{P}^j_{k|k-1}$ and $\gamma_0 = w^j_{k-1}$

3 **for** $n = 1 : n_z!$ **do**

4 Set $\hat{\mathbf{x}}^j_{k|k-1} = \boldsymbol{\mu}_0$, $\mathbf{P}^j_{k|k-1} = \boldsymbol{\Sigma}_0$ and $w^j_k = \gamma_0$

5 Initialize $\epsilon_n = 0$

6 **for** $n' = 1 : n_z$ **do**

7 Set $i = \mathbf{d}_n(n')$ and $z^i_k = \mathbf{z}_k(i)$

8 Compute $\hat{\mathbf{x}}^{i,j}_{k|k}$ and $\mathbf{P}^{i,j}_{k|k}$ using z^i_k via (20) $\sim$ (27)

9 Update the weight $w^j_k = w^j_k \mathcal{N}(z^i_k | \hat{z}^{i,j}_{k|k-1}, \mathbf{P}^{i,j}_{zz,k})$

10 Calculate the NIS (see Section IV-B) $\varphi^i_n = (z^i_k - \hat{z}^{i,j}_{k|k-1})^T (\mathbf{P}^{i,j}_{zz,k})^{-1} (z^i_k - \hat{z}^{i,j}_{k|k-1})$

11 Update $\epsilon_n = \epsilon_n + \varphi^i_n$

12 Set $\hat{\mathbf{x}}^j_{k|k-1} = \hat{\mathbf{x}}^{i,j}_{k|k}$ and $\mathbf{P}^j_{k|k-1} = \mathbf{P}^{i,j}_{k|k}$

13 **end**

14 Set $\boldsymbol{\mu}_n = \hat{\mathbf{x}}^{i,j}_{k|k}$, $\boldsymbol{\Sigma}_n = \mathbf{P}^{i,j}_{k|k}$ and $\gamma_n = w^j_k$

15 **if** $n < n_z!$ **then**

16 Permute $\mathbf{d}_n$ to produce $\mathbf{d}_{n+1}$ such that $\mathbf{d}_{n+1} \neq \mathbf{d}_{j'}, \forall j' \leq n$.

17 **end**

18 **end**

19 Find $\gamma_d = \text{argmax}\{\gamma_1, \gamma_2, \ldots, \gamma_{n_z!}\}$

20 Set $\hat{\mathbf{x}}^j_{k|k} = \boldsymbol{\mu}_d$, $\mathbf{P}^j_{k|k} = \boldsymbol{\Sigma}_d$, $w^j_k = \gamma_d$ and $\epsilon^j_k = \epsilon_d$.

We next proceed to split $\mathcal{N}(\mathbf{x}_k | \hat{\mathbf{x}}_p, \mathbf{P}_p)$ into three components such that $\mathcal{N}(\mathbf{x}_k | \hat{\mathbf{x}}_p, \mathbf{P}_p) \approx \sum_{q=1}^3 \pi_q \mathcal{N}(\mathbf{x}_k | \hat{\boldsymbol{\eta}}_q, \boldsymbol{\Omega}_q)$, where the parameters of the new components, π_q, $\hat{\boldsymbol{\eta}}_q$ and $\boldsymbol{\Omega}_q$, are listed in Table I [20]. Here, $\mathbf{e}$ is the eigenvector corresponding to the largest eigenvalue of $\mathbf{P}_p$, λ, and $\delta = 0.5$. $\pi_3 \mathcal{N}(\mathbf{x}_k | \hat{\boldsymbol{\eta}}_3, \boldsymbol{\Omega}_3)$ has the same mean vector as $w_c \mathcal{N}(\mathbf{x}_k | \hat{\mathbf{x}}^t_{k|k-1}, \mathbf{P}^t_{k|k-1})$, and they are merged to maintain that after splitting the predictive distribution, only 3 components are retained. Eventually, the predictive distribution of the tth component $\mathcal{N}(\mathbf{x}_k | \hat{\mathbf{x}}^t_{k|k-1}, \mathbf{P}^t_{k|k-1})$ is split as

$$\begin{aligned} &\mathcal{N}(\mathbf{x}_k | \hat{\mathbf{x}}^t_{k|k-1}, \mathbf{P}^t_{k|k-1}) \\ &\quad \approx w_p \pi_1 \mathcal{N}(\mathbf{x}_k | \hat{\boldsymbol{\eta}}_1, \boldsymbol{\Omega}_1) + w_p \pi_2 \mathcal{N}(\mathbf{x}_k | \hat{\boldsymbol{\eta}}_2, \boldsymbol{\Omega}_2) \\ &\quad\quad + \frac{w_c}{w_a} \mathcal{N}(\mathbf{x}_k | \hat{\boldsymbol{\eta}}_3, w_a \mathbf{P}^t_{k|k-1} + (1 - w_a) \boldsymbol{\Omega}_3) \end{aligned} \tag{30}$$

where $w_a = w_c / (w_c + w_p \pi_3)$. The three components in (30) are then updated separately using the measurement update described in Algorithm 1.

After the measurement update, the state posterior at time k can be expressed as a Gaussian mixture given in (1) with M_k ($M_k \geq N_{k-1}$) components, due to possible component splitting. The final output of the developed GMM-CQKF is the sample mean $\hat{\mathbf{x}}_{k|k}$ and sample covariance matrix $\mathbf{P}_{k|k}$, which can be computed using (4) and (3).

TABLE I

Weight	Mean	Covariance
$\pi_1 = 1/6$	$\hat{\boldsymbol{\eta}}_1 = \hat{\mathbf{x}}_p + \delta\sqrt{\lambda}\mathbf{e}$	$\boldsymbol{\Omega}_1 = \mathbf{P}_p - 1/3\delta^2\lambda\mathbf{e}\mathbf{e}^T$
$\pi_2 = 1/6$	$\hat{\boldsymbol{\eta}}_2 = \hat{\mathbf{x}}_p - \delta\sqrt{\lambda}\mathbf{e}$	$\boldsymbol{\Omega}_2 = \mathbf{P}_p - 1/3\delta^2\lambda\mathbf{e}\mathbf{e}^T$
$\pi_3 = 4/6$	$\hat{\boldsymbol{\eta}}_3 = \hat{\mathbf{x}}_p$	$\boldsymbol{\Omega}_3 = \mathbf{P}_p - 1/3\delta^2\lambda\mathbf{e}\mathbf{e}^T$

B. Innovation-based Mixture Reduction

Different from existing MR techniques such as those surveyed in Section II, the newly proposed innovation-based MR method does not attempt to constrain the number of Gaussian components under a desired value. In fact, limiting the number of components has been achieved in the measurement update, where only when the number of components is less than N_{max}, the component splitting will be performed. The aim of the proposed MR technique is to remove, from the posterior mixture distribution, the components failing to pass the innovation-based filtering consistency test. This prevents the components with relatively small weights but following the true state from being pruned or merged. As will be shown in the simulation section, this can mitigate the degrading effect of inconsistent components on the filtering accuracy.

To decide whether to eliminate the jth component, we compute the associated normalized innovation squared (NIS) [21]. Specifically, the NIS of the jth component is equal to

$$\epsilon^j_k = \sum_{i=1}^{n_z} \nu^{i,j}_k (\mathbf{P}^{i,j}_{zz,k})^{-1} (\nu^{i,j}_k)^T \tag{31}$$

where $\nu^{i,j}_k = z^i_k - \hat{z}^{i,j}_{k|k-1}$ is the measurement innovation and $\mathbf{P}^{i,j}_{zz,k}$ is its covariance matrix. In fact, ϵ^j_k is calculated during the measurement update ordering process (see lines 10-11 in Algorithm I). It is known that when the filtering is consistent, ϵ^j_k should follow a chi-squared distribution with n_z degrees of freedom (i.e, $\epsilon^j_k \sim \chi^2_{n_z}$).

To account for the filtering history, the jth component that satisfy (32) is removed

$$\sum_{k'=k-N_T+1}^{k} \epsilon^j_{k'} > \chi^2_{N_T n_z}(1 - \alpha) \tag{32}$$

where $\chi^2_{N_T n_z}(1-\alpha)$ is the $100(1-\alpha)$ percentile point of the chi-squared distribution with $N_T n_z$ degrees of freedom. N_T determines the memory length of the consistency test.

It is possible that after the innovation-based pruning, the remaining number of components is smaller than a prespecified threshold N_{min}, which may lead to a poor coverage of the state space. In this case, we choose to keep all the components.

V. SIMULATIONS

This section evaluates the performance of GMM-CQKF in a nonlinear target tracking problem. We shall demonstrate the advantage of using the proposed measurement update ordering

and innovation-based MR technique in improving the target tracking accuracy.

A. Tracking Scenario

Consider a three-dimensional (3D) target tracking scenario where TDOA and FDOA measurements observed by a pair of UAVs are used for estimating target trajectory. The target has a known altitude $h = 20$km. Its position and velocity at time k are denoted as $\mathbf{u}_k = [x_k, y_k, h]^T$ and $\dot{\mathbf{u}}_k = [\dot{x}_k, \dot{y}_k, 0]^T$. This indicates that the target is moving in a plane that is parallel to and 20km above the x-y plane. The target trajectory follows

$$\mathbf{x}_k = \mathbf{F}_k \mathbf{x}_{k-1} + \mathbf{n}_k. \tag{33}$$

$\mathbf{x}_k = [x_k, y_k, \dot{x}_k, \dot{y}_k]^T$ is the target kinematic state at time k to be identified. $\mathbf{F}_k$ is the state transition matrix and $\mathbf{Q}_k$ is the covariance matrix of the process noise $\mathbf{n}_k$. They are given by

$$\mathbf{F}_k = \begin{bmatrix} 1 & 0 & T & 0 \\ 0 & 1 & 0 & T \\ 0 & 0 & 1 & 0 \\ 0 & 0 & 0 & 1 \end{bmatrix}, \quad \mathbf{Q}_k = q \begin{bmatrix} \frac{T^4}{4} & 0 & \frac{T^3}{2} & 0 \\ 0 & \frac{T^4}{4} & 0 & \frac{T^3}{2} \\ \frac{T^3}{2} & 0 & T^2 & 0 \\ 0 & \frac{T^3}{2} & 0 & T^2 \end{bmatrix}$$

where $T = 3$s is the sampling period and $q = 10^{-4}\text{m}^2/\text{s}^4$ is the process noise intensity.

There are $n_z = 2$ measurements observed at each sampling time k and they are collected in $\mathbf{z}_k = [z_k^1, z_k^2]^T$. The first measurement $z_k^1 = h_k^1(\mathbf{x}_k) + v_k^1$ is the TDOA of the target signal received at the two UAVs. The measurement noise v_k^1 is assumed to be Gaussian with zero mean and standard deviation $\sigma_{1,k} = 40$ns. The true TDOA $h_k^1(\mathbf{x}_k)$ is equal to

$$h_k^1(\mathbf{x}_k) = \frac{1}{c}(\|\mathbf{u}_k - \mathbf{s}_k^{(2)}\| - \|\mathbf{u}_k - \mathbf{s}_k^{(1)}\|)$$

where c is the signal propagation speed, $\| * \|$ represents the Euclidean norm and $\mathbf{s}_k^{(g)}$ $(g = 1, 2)$ are the known positions of the two UAVs at time k. $z_k^2 = h_k^2(\mathbf{x}_k) + v_k^2$ is the FDOA measurement and its true value is

$$h_k^2(\mathbf{x}_k) = \frac{f_0}{c}[\mathbf{e}_k^{(2)T}(\dot{\mathbf{u}}_k - \dot{\mathbf{s}}_k^{(2)}) - \mathbf{e}_k^{(1)T}(\dot{\mathbf{u}}_k - \dot{\mathbf{s}}_k^{(1)})].$$

$f_0 = 1$GHz is the carrier frequency of the target signal, $\dot{\mathbf{s}}_k^{(g)}$ $(g = 1, 2)$ are velocities of the two UAVs at time k and $\mathbf{e}_k^{(g)} = (\mathbf{u}_k - \mathbf{s}_k^{(g)})/\|\mathbf{u}_k - \mathbf{s}_k^{(g)}\|$ is the unit vector from UAV g to the target position $\mathbf{u}_k$. The FDOA noise v_k^2 is assumed to be Gaussian with zero mean and standard deviation $\sigma_{2,k} = 5$Hz. We further assume that v_k^1 and v_k^2 are uncorrelated and they are both independent of the process noise $\mathbf{n}_k$.

B. Performance Metrics

We quantify the tracking performance using the root mean square error (RMSE) of the target position estimates from simulations, which is defined as

$$\text{RMSE}(\mathbf{u}_k) = \sqrt{\frac{1}{M_c}\sum_{i'=1}^{M_c}(x_k - \hat{x}_k^{i'})^2 + (y_k - \hat{y}_k^{i'})^2}$$

where $[\hat{x}_k^{i'}, \hat{y}_k^{i'}]^T$ is the target position estimate in the i'th ensemble run and $M_c = 500$ is the number of ensemble runs.

The posterior Cramér-Rao Lower Bound (pCRLB) gives the best tracking performance we can achieve. Denoting $\mathbf{A}[i, j]$ as the element in the ith row and jth column of matrix $\mathbf{A}$, the pCRLB for the target position estimate at time k is

$$\text{pCRLB}(\mathbf{u}_k) = \sqrt{\mathbf{J}_k^{-1}[1,1] + \mathbf{J}_k^{-1}[2,2]}$$

The information matrix $\mathbf{J}_k$ for the considered tracking problem can be calculated recursively via [1], [22]

$$\mathbf{J}_k = (\mathbf{F}_k \mathbf{J}_{k-1}^{-1} \mathbf{F}_k^T + \mathbf{Q}_k)^{-1} + \mathbf{H}_k^T \mathbf{R}_k^{-1} \mathbf{H}_k$$

where $\mathbf{R}_k = \text{diag}\{c^2\sigma_{1,k}^2, (c/f_0)^2\sigma_{2,k}^2\}$ is the measurement noise covariance. $\mathbf{H}_k$ is the Jacobian matrix equal to

$$\mathbf{H}_k^T = \begin{bmatrix} \mathbf{e}_k^{(2)}(1) - \mathbf{e}_k^{(1)}(1) & \boldsymbol{\phi}_k^{(2)}(1) - \boldsymbol{\phi}_k^{(1)}(1) \\ \mathbf{e}_k^{(2)}(2) - \mathbf{e}_k^{(1)}(2) & \boldsymbol{\phi}_k^{(2)}(2) - \boldsymbol{\phi}_k^{(1)}(2) \\ 0 & \mathbf{e}_k^{(2)}(1) - \mathbf{e}_k^{(1)}(1) \\ 0 & \mathbf{e}_k^{(2)}(2) - \mathbf{e}_k^{(1)}(2) \end{bmatrix}$$

$\boldsymbol{\phi}_k^{(g)} = (\mathbf{s}_k^{(g)} - \mathbf{u}_k)\dot{r}_k^g/(r_k^g)^2 + (\dot{\mathbf{u}}_k - \dot{\mathbf{s}}_k^{(g)})/r_k^g$, $r_k^g = \|\mathbf{u}_k - \mathbf{s}_k^{(g)}\|$ and $\dot{r}_k^g = \mathbf{e}_k^{(g)T}(\dot{\mathbf{u}}_k - \dot{\mathbf{s}}_k^{(g)})$. We assume a non-informative prior for the state estimate such that $\mathbf{J}_k$ is initialized with $\mathbf{J}_1 = \mathbf{H}_1^T \mathbf{R}_1^{-1} \mathbf{H}_1$.

C. Implementation Details

In the simulation experiments, we set the GMM-CQKF filter to initially have $N_1 = 6$ components. The TDOA measurement z_1^1 obtained at time 1 is used to initialize them. In particular, we adopt the GMM representation of the TDOA measurement developed in [5] for component initialization. The generated components are assigned weights equal to $w_1^j = 1/N_1$.

Note from (29) that the scalar κ is required to determine the covariance matrix $\mathbf{P}_p$ in $\mathcal{N}(\mathbf{x}_k|\hat{\mathbf{x}}_p, \mathbf{P}_p)$. This distribution will be split to improve the coverage of the part of the state space originally covered by the component with the largest weight in the mixture, $\mathcal{N}(\hat{\mathbf{x}}_k|\hat{\mathbf{x}}_{k|k-1}^t, \mathbf{P}_{k|k-1}^t)$. Let $\boldsymbol{\mu}_j$ be the first two elements of $\hat{\mathbf{x}}_{k|k-1}^j$ and $\boldsymbol{\Sigma}_j$ be the 2×2 upper left block of $\mathbf{P}_{k|k-1}^j$. Suppose $\mathcal{N}(\hat{\mathbf{x}}_k|\hat{\mathbf{x}}_{k|k-1}^r, \mathbf{P}_{k|k-1}^r)$ is the component whose mean vector has the smallest Euclidean distance to $\hat{\mathbf{x}}_{k|k-1}^t$. κ is thus obtained via

$$\kappa = \max\{\frac{1}{\sqrt{\lambda_t}}\boldsymbol{\rho}_t^T(\boldsymbol{\mu}_t - \boldsymbol{\mu}_r), 1\}$$

where $\boldsymbol{\rho}_t$ is the eigenvector of $\boldsymbol{\Sigma}_t$ corresponding to its largest eigenvalue λ_t.

D. Results

The simulated target tracking scenario is depicted in Fig. 1. The target moves with an initial speed of 125m/s to the left and its position at time 1 is $\mathbf{u}_1 = [58.1434, 159.7477, 20]^T$km. The two UAVs have parallel trajectories with a speed of 150m/s and they maintain a fixed distance of 25km from each other such that $\mathbf{s}_k^{(2)} - \mathbf{s}_k^{(1)} = [25, 0, 0]^T$km and $\dot{\mathbf{s}}_k^{(2)} = \dot{\mathbf{s}}_k^{(1)}$. They both move with a constant turn rate of 0.05rad/s. They would

change their turn directions when crossing the line $y = 3$km. The two UAVs have an altitude of 5km and at time 1, UAV 1 is located at $\mathbf{s}_1^{(1)} = [-12.5, 0, 5]^T$km and moving with a velocity of $\dot{\mathbf{s}}_1^{(1)} = [150, 0, 0]^T$m/s.

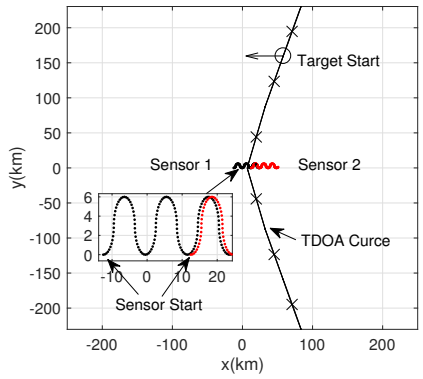

Fig. 1. The TDOA and FDOA target tracking scenario, the cross $\times$ on the TDOA curve denotes the mean of a mixture component after initialization.

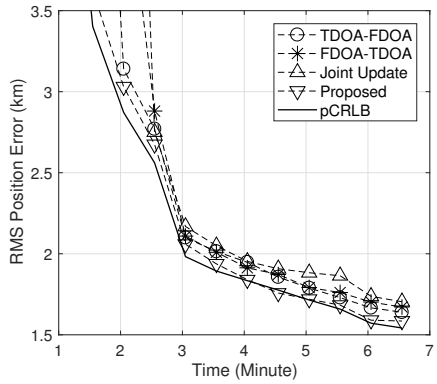

Fig. 2. Target position RMSE of the GMM-CQKF filter with different measurement update ordering schemes.

The first simulation experiment evaluates the performance of the GMM-CQKF with different measurement update ordering schemes. The results are summarized in Fig. 2, where the target position RMSE is plotted as a function of time. Besides the proposed ordering technique in Section IV.A, we consider other three strategies. They include performing TDOA update first (denoted as TDOA-FDOA), performing FDOA update first (denoted as FDOA-TDOA) and joint exploration of TDOA and FDOA (denoted as TDOA+FDOA).

The GMM-CQKF is realized with parameters set to be $n_d = 3$, $N_{\max} = 16$, $N_{min} = 3$, $w_p = 10^{-4}$, $\alpha = 0.01$ and $N_T = 3$. It can be seen from Fig. 2 that these four ordering methods provide comparable target position RMSEs close to the pCRLB. Among them, the estimation accuracy from jointly exploiting the TDOA and FDOA in the measurement update is the worst. Performance improvement can be obtained when the measurements are used in sequence, because measurement update in a sequential manner may reduce the nonlinearity in the measurement update stage. The proposed measurement update ordering, which selects the ordering to maximize the component weight, offers the best performance, as expected.

In the second simulation, we compare the performance of the GMM-CQKF with various MR techniques. The simulated scenario is different from that shown in Fig. 1 in three aspects: 1) the target moves to the right; 2) the two UAVs now have a smaller turn rate of 0.0064rad/s and they do not change their turn directions during the whole tracking process; 3) UAV 1 has an initial velocity of $\dot{\mathbf{s}}_1^{(1)} = [127.1997, -79.4998, 0]^T$m/s. The parameters for implementing the GMM-CQKF are the same as those used to generate Fig. 2, except that here, we set the maximum number of components to $N_{max} = 6$. For a fair comparison, the realized GMM-CQKFs have the same measurement update ordering and component splitting strategies, as detailed in Section IV. A. We change the simulation scenario so that the target position RMSE would converge slower than in the first simulation, which could better demonstrate the effect of different MR techniques on the tracking performance.

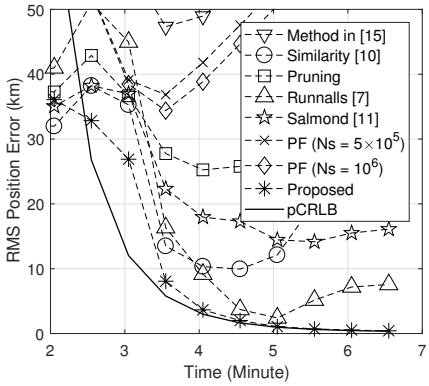

Fig. 3. Target position RMSE of the GMM-CQKF filter with different MR techniques.

The obtained results are summarized in Fig. 3, where the target position RMSEs of the GMM-CQKF with different MR techniques are plotted as a function of time. The results from bootstrap PFs with different number of particles are also shown. We can see that the pruning method, which removes the components with lowest weights to fix the number of components at N_{max}, and the MR technique from [14] have poor performance. This is because the pruning method may mistakenly eliminate component following the true target trajectory. Moreover, the technique from [14] could introduce significant errors due to merging components distant from each other. Although the similarity-based method from [9] exhibits fast convergence, its target position RMSE increases drastically after 5 minutes, possibly due to that it does not consider the component weights when merging them. On the contrary, MR methods such as the KL-based method [6] and joining method [10] merge components that have small weights, close mean vectors and similar covariances perform better. But they are still inferior to the proposed MR technique that is based on innovation process and takes into

account the filtering history. This clearly demonstrates the advantage of removing inconsistent components in improving the tracking accuracy. The bootstrap PFs, on the other hand, even with a large number of 10^6 particles, yield unsatisfactory performance probably due to the lack of particle diversity.

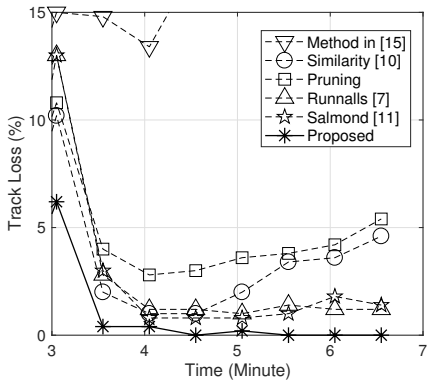

Fig. 4. Track loss probability of the GMM-CQKF filter with different MR techniques.

Fig. 4 shows the track loss probabilities of the GMM-CQKF filter when using different MR methods as a function of time. We declare the filter to have a track loss if its position estimation error is larger than $4 \cdot$ pCRLB. The observations are very similar to those obtained from Fig. 3. The proposed innovation-based MR method provides the lowest track loss probability. The underlying reason is that the component following the true target track is likely to be consistent and it would not be eliminated by the proposed MR technique. Therefore, the probability that the GMM-CQKF can converge to a solution close to the true target trajectory is increased.

VI. Conclusions

In this paper, we integrated the GMM framework with a recently developed nonlinear KF and established GMM-CQKF, a new filter capable of handling nonlinear and non-Gaussian filtering problems. Two enhancements were introduced. The first enhancement is to determine the optimal measurement update order for each component in the GMM-CQKF by selecting the one that maximizes the component weight. The second enhancement is an innovation-based MR technique that also takes into account the filtering history of a component when deciding whether it is about to be removed from the posterior mixture. Simulations using a nonlinear TDOA and FDOA tracking problem verified that significantly improved target tracking accuracy close to the pCRLB can be obtained with GMM-CQKF with the two proposed enhancements over GMM-CQKF with other measurement update ordering and MR strategies. These two enhancements may be incorporated into other GMM-based filtering techniques for performance improvement.

Acknowledgment

The work of Le Yang has been supported by the Natural Science Foundation of China under Grant no. 61304264. The work of Min Zhang has been supported by the National Defence Science and Technology Project Foundation of China under Grant no. 3101140.

References

[1] B. Ristic, S. Arulampalam, and N. Gordon, *Beyond the Kalman filter: Particle filters for tracking applications*. Boston MA: Artech House, 2004.

[2] P. Rebeschini and R. V. Handel, "Can local particle filters beat the curse of dimensionality?" *The annals of applied probability*, vol. 25, no. 5, pp. 2809–2866, 2015.

[3] I. Arasaratnam, S. Haykin, and R. J. Elliott, "Discrete-time nonlinear filtering algorithms using Gauss-Hermite quadrature," *Proc. IEEE*, vol. 95, no. 5, pp. 953–977, May. 2007.

[4] I. Arasaratnam and S. Haykin, "Cubature Kalman filters," *IEEE Trans. Autom. Control*, vol. 54, no. 6, pp. 1254–1269, Jun. 2009.

[5] D. Musicki, R. Kaune, and W. Koch, "Mobile emitter geolocation and tracking using TDOA and FDOA measurements," *IEEE Trans. Signal Process.*, vol. 58, no. 3, pp. 1863–1874, Mar. 2010.

[6] A. R. Runnalls, "Kullback-Leibler approach to Gaussian mixture reduction," *IEEE Trans. Aerosp. Electron. Syst.*, vol. 43, no. 3, pp. 989–999, Jul. 2007.

[7] S. Bhaumik and Swati, "Cubature quadrature Kalman filter," *IET Signal Process.*, vol. 7, pp. 533–541, Sept. 2013.

[8] L. Y. Pao, "Multisensor multitarget mixture reduction algorithms for tracking," *Journal of Guidance, Control, and Dynamics*, vol. 17, no. 6, pp. 1205–1211, 1994.

[9] F. Faubel, J. McDonough, and D. Klakow, "The split and merge unscented Gaussian mixture filter," *IEEE Signal Process. Lett.*, vol. 16, no. 9, pp. 786–789, Sep. 2009.

[10] D. J. Salmond, "Mixture reduction algorithms for target tracking," in *IEE Colloq. State Estim. Aerosp. and Tracking Appl.*, Dec. 1989, pp. 1–4.

[11] J. L. Williams and P. S. Maybeck, "Cost-function-based Gaussian mixture reduction for target tracking," in *Proc. 6th Int. Conf. Inf. Fusion (FUSION)*, vol. 2, Cairns, Queensland, Australia, Jul. 2003, pp. 1047–1054.

[12] T. Ardeshiri, U. Orguner, C. Lundquist, and T. B. Schön, "On mixture reduction for multiple target tracking," in *Proc. 15th Int. Conf. Inf. Fusion (FUSION)*, Singapore, Singapore, Jul. 2012, pp. 692–699.

[13] J. E. Harmse, "Reduction of Gaussian mixture models by maximum similarity," *Journal of Nonparametric Statistics*, vol. 22, no. 6, pp. 703–709, 2010.

[14] P. H. Leong, S. Arulampalam, T. A. Lamahewa, and T. D. Abhayapala, "A Gaussian-sum based cubature Kalman filter for bearings-only tracking," *IEEE Trans. Aerosp. Electron. Syst.*, vol. 49, no. 2, pp. 1161–1176, Apr. 2013.

[15] D. Schieferdecker and M. F. Huber, "Gaussian mixture reduction via clustering," in *Proc. 12th Int. Conf. Inf. Fusion (FUSION)*, Seattle, WA, USA, Jul. 2009, pp. 1536–1543.

[16] M. F. Huber and U. D. Hanebeck, "Progressive Gaussian mixture reduction," in *Proc. 11th Int. Conf. Inf. Fusion (FUSION)*, Cologne, Germany, Jul. 2008, pp. 1–8.

[17] D. F. Crouse, P. Willett, K. Pattipati, and L. Svensson, "A look at Gaussian mixture reduction algorithms," in *Proc. 14th Int. Conf. Inf. Fusion (FUSION)*, Chicago, IL, USA, Jul. 2011, pp. 1–8.

[18] B. Jia, M. Xin, and Y. Cheng, "High-degree cubature Kalman filter," *Autom.*, vol. 49, no. 2, pp. 510–518, Feb. 2013.

[19] S. Khalid, N. Rehman, and S. Abrar, "Higher-degree stochastic integration filtering," *arXiv preprint*, pp. 1–5, Aug. 2016, available at: arxiv.org/abs/1608.00337.

[20] P. H. Leong, S. Arulampalam, T. A. Lamahewa, and T. D. Abhayapala, "Gaussian-sum cubature Kalman filter with improved robustness for bearings-only tracking," *IEEE Signal Process. Lett.*, vol. 21, no. 5, pp. 513 – 517, May. 2014.

[21] Y. Bar-Shalom, X. R. Li, and T. Kirubarajan, *Estimation with applications to tracking and navigation: theory algorithms and software*. New York: Wiley, 2001.

[22] P. Tichavsky, C. H. Muravchik, and A. Nehorai, "Posterior Cramér-Rao bounds for discrete-time nonlinear filtering," *IEEE Trans. Signal Process.*, vol. 46, no. 5, pp. 1386–1396, May. 1998.